Journal of Photochemistry and Photobiology A: Chemistry 217 (2011) 147–156

Contents lists available at ScienceDirect

Journal of Photochemistry and Photobiology A: Chemistry

journal homepage: www.elsevier.com/locate/jphotochem

Synthesis and fluorescence characteristics of novel asymmetric cyanine dyes for DNA detection

Stefka Kaloyanova[a,1], Valeriya M. Trusova[b,1], Galyna P. Gorbenko[b], Todor Deligeorgiev[a,*]

[a] Department of Applied Organic Chemistry, Faculty of Chemistry, University of Sofia, 1 James Bourchier Ave., 1164 Sofia, Bulgaria
[b] Department of Biological and Medical Physics, V.N. Karazin Kharkov National University, 4 Svobody Sq., Kharkov 61077, Ukraine

ARTICLE INFO

Article history:
Received 20 July 2010
Received in revised form
18 September 2010
Accepted 2 October 2010
Available online 29 October 2010

Keywords:
New cyanine dyes
DNA
Binding parameters
Fluorescence

ABSTRACT

Sixteen new asymmetric monomethine cyanine dyes have been synthesized and their spectral characteristics and interaction with double stranded DNA have been investigated. The dyes absorb in the region 453–519 nm and have molar absorptivities in the range 37.900–93.100 l M^{-1} cm^{-1}. The dyes do not have intrinsic fluorescence, but in the presence of dsDNA they exhibited a significant enhancement in fluorescence. The most pronounced increase was found for **D9**, **D10**, **D12** and **D16** allowing the recommendation of these dyes as the most sensitive DNA markers. Thermodynamic analysis of cyanine–DNA complexation was carried out using the McGhee & von Hippel non-cooperative excluded site model, and binding parameters have been derived. A hypothesis describing the DNA–dye binding mode has been proposed.

1. Introduction

Rapid and highly sensitive quantitative detection of DNA is crucial in many medical, biological and biotechnological applications. The most important techniques include the polymerase chain reaction, DNA sequencing, DNA library development, agarose gel and capillary electrophoresis staining, DNA damage detection, purification of DNA fragments for subcloning, the identification of contaminating DNA in recombinant protein products, flow cytometry and the evaluation of biological activity [1]. Since the intrinsic emission of nucleic acids is very weak, extrinsic fluorescent probes and labels are generally used for DNA recognition. A wide range of fluorophores, including ethidium bromide [2], Hoechst 33258 [3], acridine orange [4], proflavine (acridine-3,6-diamine) [5], DAPI (4′,6-diamidino-2-phenylindole) [6] have been employed to identify DNA [7]. However, these reported molecules suffer from one severe drawback—they are highly emissive in solution thereby creating a strong background signal. This disadvantage stimulated the search for novel fluorescent probes which could provide an adequate alternative to the classical fluorphores. Ideally, a DNA-specific dye should readily switch between nonemissive and emissive states upon binding to nucleic acids. The most promising dyes with these characteristics are cyanine dyes which display the light-up effect (strong increase in fluorescence intensity) when interacting with nucleic acids [8]. Cyanine dyes are photosensitive structures composed of two quaternized, nitrogen-containing, heterocyclic ring structures, that are linked through a polymethine bridge [1]. The dyes show large extinction coefficients and a strong π–π^* absorption which can be easily tuned from the visible to the NIR region by synthesizing structural modifications in the chromophore moiety. This superior property of cyanine dyes allows them to be programmed in order to achieve the desired functional fluorescent nanomaterials for DNA visualization. Furthermore, cyanine dyes without intrinsic fluorescence in solution have a high binding affinity to nucleic acids and illuminate only after binding to a substrate. The modification of benzazole heterocyclic moieties in cyanine dye structures influences the kind of interaction they have with nucleic acids [9,10]. The substituents at position 6 of the benzothiazole moiety impart a crescent shape to the dye molecule, particularly the benzoylamino group, thus creating a preference for minor groove-binding [11].

In attempting to broaden the molecular library of known DNA reporter molecules, we directed our efforts towards the synthesis and characterization of a range of asymmetric cyanine dyes differing in their structural features and spectroscopic behaviour. More specifically, our goals were: (i) to synthesize novel asymmetric analogues of Thiazole Orange with amide substituents in the benzothiazole moiety; (ii) to identify spectroscopically those fluorophores that would posses the highest sensitivity to dsDNA; (iii) to describe DNA–cyanine complexation thermodynamically.

* Corresponding author. Tel.: +359 2 8161269; fax: +359 2 9625438.
E-mail address: toddel@chem.uni-sofia.bg (T. Deligeorgiev).
[1] Both authors contributed equally.

1010-6030/$ – see front matter © 2010 Elsevier B.V. All rights reserved.
doi:10.1016/j.jphotochem.2010.10.002

2. Materials and methods

2.1. Materials

Cattle spleen DNA was obtained from Reakhim (Russia) and salmon testes DNA was obtained from Sigma–Aldrich. Tris–HCl and EDTA were obtained from Sigma (St. Louis, MO, USA). All other starting materials and solvents were commercial products of analytical grade (Sigma–Aldrich or TCI Europe) and were used without further purification.

2.2. Analysis methods and equipment

^{1}H NMR spectra were recorded on a Brucker Avance II 600 MHz instrument in DMSO-d_6. Elemental analyses were performed on a Vario III instrument. Melting points were determined on a Köfler apparatus and are uncorrected. Absorption spectra were obtained on a Unicam UV 500 spectrophotometer in methanol (1×10^{-5} mol/l). Fluorescence measurements were taken on PerkinElmer LS45 and LS55 spectrofluorimeters.

2.3. Synthesis of cyanine dyes D1-D16

In a reaction vessel equipped with magnetic stirrer equimolar amounts of intermediates **5a**–**5d** (0.001 mol) and **8a**–**8g**, **10a** or **10b** (0.001 mol) were suspended or dissolved in 10 ml ethanol (dyes **D2**–**D5**, **D7**–**D9**) or 3 ml acetic anhydride (dyes **D1**, **D6**, **D10**–**D16**). N-diisopropylethylamine (0.002 mol) (for **D13** 0.003 mol) was added and the reaction mixture was stirred at room temperature for 1–5 h. The progress of the reaction was monitored by TLC (Merck F 254 silica gel; dichloromethane:methanol:acetic acid 86:13:1). The resulting precipitate was filtered off, washed with diethyl ether and air-dried. For compounds **D1**, **D6**, **D10**–**D16** when acetic anhydride was used as reaction media—diethyl ether was added to the reaction mixture and the precipitated dye was filtered off and air-dried. Dyes **D1**–**D16** were recrystallized from methanol.

2.4. Preparation of dye and DNA solutions

Stock solutions of dyes were prepared by dissolving the dyes in ethanol to achieve final concentrations of ~10 μM (1×10^{-5} M). DNA solutions were prepared in 10 mM Tris–HCl, 0.5 mM EDTA buffer, pH 7.4. The concentrations of cyanines and nucleic acid were determined spectrophotometrically using their extinction coefficients and $\varepsilon_{260} = 6.4 \times 10^3$ M^{-1} cm^{-1} for DNA. The extinction coefficients of the dyes are given in Table 3.

To determine the fluorescence spectra of dsDNA–dye complexes, appropriate amounts of a stock solution of salmon sperm dsDNA in 10 mM Tris–HCl, 0.5 mM EDTA buffer, pH 7.4 (TE buffer) with a concentration 50 μg/ml, was added to each dye in TE buffer. Dye stock solutions with a concentration 1×10^{-4} M were prepared in DMSO and these were diluted with TE buffer. The final DNA concentration was 1×10^{-6} M b.p. (8 μg/ml) and the final dye concentration was 1×10^{-7} M, yielding a molar ratio of dsDNA bp - dye of 10:1. The mixtures were incubated at room temperature for 15 min prior to spectroscopic measurement.

2.5. Fluorescence measurements

Fluorescence measurements were performed in 10 mM Tris–HCl, 0.5 mM EDTA buffer, pH 7.4 at room temperature using 10-mm path-length quartz cuvettes in a Perkin Elmer LS55 spectrofluorimeter equipped with a magnetically stirred, thermostated cuvette holder (Perkin-Elmer Ltd., Beaconsfield, UK). Excitation and emission slit widths were set at 10 nm.

Fluorescence spectra to determine the fluorescence intensity of the dye solutions after binding to dsDNA (salmon sperm, Sigma–Aldrich) were scanned on a Perkin Elmer LS45 fluorescence spectrometer in 10 mM Tris–HCl, 0.5 mM EDTA buffer, pH 7.4 at room temperature.

2.6. Binding model

Thermodynamic analysis of DNA–cyanine complexation was made in terms of the McGhee & von Hippel excluded site model allowing calculation of the binding constant and the stoichiometry [12]:

$$\frac{B}{F} = KP\left(1 - \frac{nB}{P}\right)\left[\frac{1-(nB/P)}{1-(n-1)(nB/P)}\right]^{n-1} \quad (1)$$

where B and F are concentrations of bound and unbound dye, respectively, P is DNA concentration, K association constant, n represents the site exclusion parameter (i.e. number of DNA base pairs covered by one dye molecule). The values of K and n were estimated using the nonlinear least-square fitting procedure.

3. Results and discussion

3.1. Synthesis and structural analysis of dyes *D1–D16*

Monomethine cyanine dyes are generally synthesized by the reaction of two heterocyclic quaternary salts, bearing respectively an alkylthio and a methyl group [13].

Intermediates **5a**–**5d** were prepared according to the reported procedures [14–17] (Scheme 1).

Intermediates **8a**–**8g** and **10a**, **10b** were synthesized by quaternization of 4-methylquinoline (**6**) and 4-methylpyridine (**7**) under solvent-free conditions with the corresponding alkyl and aralkyl bromides and iodides (Schemes 2 and 3).

All intermediates are hygroscopic and their structures were proved along with the structures of the dyes by ^{1}H NMR spectroscopy and elemental analyses.

The series of novel monomethine cyanine dyes were synthesized in good to high yields and high purity by condensation of quaternized 4-methylqunolinium or 4-methylpyridinium salts with quaternized 2-methylthioheterocyclic salts in the presence of a basic agent (N-diisopropylethylamine) and appropriate solvent, ethanol or acetic anhydride, at room temperature (Scheme 4). The dyes obtained were isolated as crude products by direct filtration in the cases where ethanol was the reaction solvent. When acetic anhydride was used as reaction solvent the dyes were isolated by precipitation with diethyl ether followed by filtration.

Dyes **D1**–**D16** were recrystallized from methanol to obtain the analytical samples. The structures of the novel analogues of Thiazole Orange were evaluated by ^{1}H NMR spectroscopy (Table 1) and elemental analysis (Table 2). Reaction yields and melting points of the products are summarized in Table 2.

As seen in Scheme 4 and Table 1, the cyanines under investigation are asymmetric monomethine dyes, containing a benzothiazole fragment. The dyes are cationic in nature due to the delocalized positive charge of the chromophore. The dyes display strong absorption in the range of 453–519 nm and have molar absorptivities in the range 37.900–93.100 l M^{-1} cm^{-1}.

3.2. Fluorescence of the free dyes and after binding to dsDNA

Detailed studies of the photo-physical properties of dyes **D1**–**D16** in the presence of dsDNA (salmon testes) were made

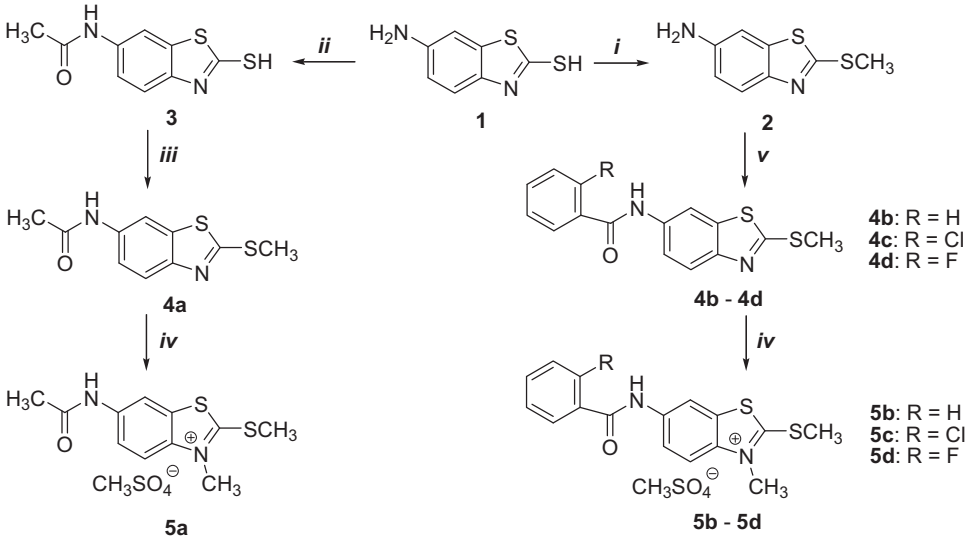

i : acetone, N-diisopropylethylamine, CH_3I, 15 *min*, r.t., 79% yield [13] ***ii*** : $(CH_3CO)_2O$, H_2SO_4, 30 *min*, reflux, 89% yield [14a] ***iii*** : H_2O/NaOH, dimethyl sulfate (DMS), 1.5 *h*, r.t., 97% yield [15] ***iv*** : trichloroethylene, DMS, 30 *min*, reflux, 60-94% yield [16] **v** : benzoyl chloride (**5b**) or 2-chlorobenzoyl chloride (**5c**) or 2-fluorobenzoyl chloride (**5d**), EtOH/NaOH, 2 *h*, r.t., 75% [14b]

Scheme 1. Synthesis of intermediated **5a**-**5d**.

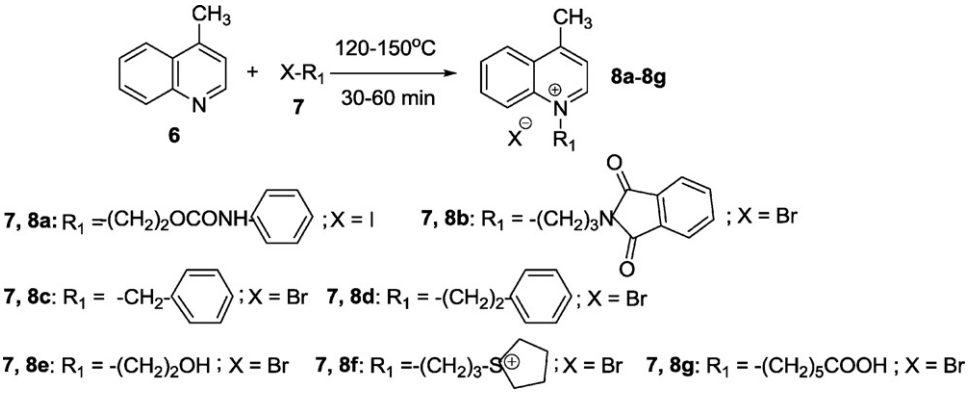

Scheme 2. Synthesis of intermediates **8a**–**8g**.

(Table 3). The dyes do not have any or have only a negligible fluorescence in TE buffer in the absence of dsDNA.

In the presence of dsDNA all dyes show enhanced fluorescence (Fig. 1). The maximal fluorescence increase was obtained at a dsDNA concentration of 8 μg/ml. Comparison of spectral properties of free and dsDNA-bound dyes under the same experimental conditions [18] revealed that the most pronounced fluorescence increase is observed in **D9**, **D10**, **D12**, **D16** (Table 3). The enhancement of cyanine fluorescence in a DNA scaffold is generally attributed to the hindered torsional rotation around the methane bridge, which results in the reduction of non-radiative relaxation of the excited state [1].

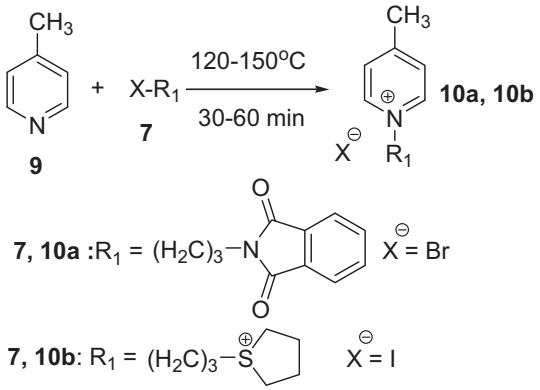

Scheme 3. Synthesis of intermediates **10a** and **10b**.

3.3. Binding studies

To derive the parameters of cyanine–DNA binding, the solutions of cyanine dyes were titrated with cattle spleen dsDNA (Fig. 2).

The experimental dependencies of dye fluorescence increase upon binding to DNA (ΔI) as a function of DNA base pairs-to-dye molar ratio (P/D) (Fig. 3). These have been analyzed in terms of the McGhee & von Hippel excluded site model (Eq. (1)). The results obtained are summarized in Table 4.

The association constants were shown to have magnitudes of 10^4–10^5, suggesting that the cyanines examined bind strongly to DNA. The molar fluorescence (a) and site exclusion parameter, i.e. number of DNA units occluded by the cyanine molecule, also have values typical of DNA–dye complexation. Interestingly, the correlation between variations in fitting parameters (K, n and a) depending on dye structure was not found. Thus, **D12** exhibited

Table 1
Structures, ^{1}H NMR analysis, absorption maxima and extinction coefficients in methanol (1×10^{-5} M) of dyes **D1**–**D16**.

Dye structures	^{1}H NMR, 600 MHz, DMSO-d_6 δ [ppm]	λ_{max} [nm]	ε [l mol^{-1} cm^{-1}]
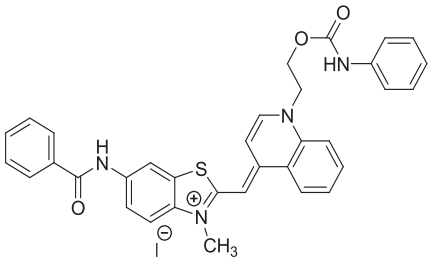 **D1**	4.03 (s, 3H, NCH_3), 4.56 (t, 2H, NCH_2), 4.90 (t, 2H, CH_2O), 6.90 (s, 1H, CH), 6.96 (t, 1H, ArH), 7.23 (t, 2H, ArH), 7.28 (d, 1H, ArH), 7.36 (s, 2H, ArH), 7.57 (t, 2H, ArH), 7.63 (t, 1H, ArH), 7.73 (t, 1H, ArH), 7.81 (d, 1H, ArH), 7.88 (d, 1H, ArH), 7.95–8.00 (m, 3H, ArH), 8.18 (d, 1H, ArH), 8.49 (brs, 1H, ArH), 8.58 (s, 1H, ArH), 8.77 (d, 1H, ArH), 9.71 (s, 1H, NH), 10.59 (s, 1H, NH)	519	70,300
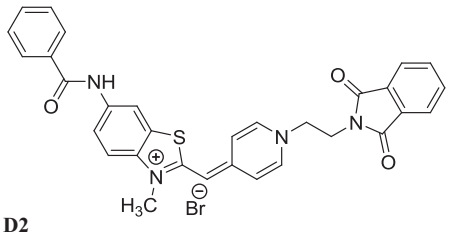 **D2**	3.73 (s, 3H, NCH_3), 4.05 (t, 2H, NCH_2), 4.44 (t, 2H, CH_2N), 6.20 (s, 1H, CH), 7.28 (d, 2H, ArH), 7.50–7.63 (m, 4H, ArH), 7.80–7.85 (m, 5H, ArH), 7.99 (d, 2H, ArH), 8.33 (d, 2H, ArH), 8.43 (d, 1H, ArH), 10.54 (s, 1H, NH)	464	37,900
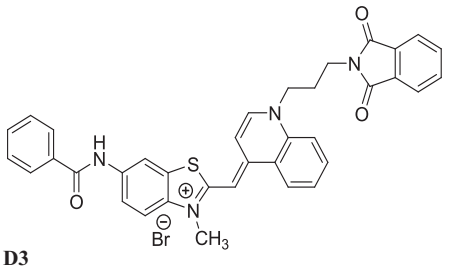 **D3**	2.06 (t, 2H, CH_2), 3.59 (t, 2H, CH_2), 3.85 (s, 3H, NCH_3), 4.50 (t, 2H, CH_2), 6.71 (s, 1H, CH), 7.13 (d, 1H, ArH), 7.37–7.47 (m, 4H, ArH), 7.66–7.73 (m, 6H, ArH), 7.82 (d, 3H, ArH), 8.00 (d, 1H, ArH), 8.42–8.45 (m, 2H, ArH), 8.59 (d, 1H, ArH), 10.44 (s, 1H, NH)	518	81,100
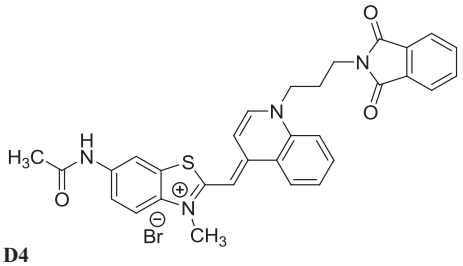 **D4**	2.10 (s, 3H, CH_3CO), 2.22 (t, 2H, CH_2), 3.75 (t, 2H, NCH_2), 4.00 (s, 3H, NCH_3), 4.66 (t, 2H, CH_2N), 6.87 (s, 1H,CH), 7.27 (d, 1H, ArH), 7.65 (dd, 1H, ArH), 7.71–7.77 (m, 2H, ArH), 7.83–7.85 (m, 2H, ArH), 7.87–7.89 (m, 2H, ArH), 7.97 (t, 1H, ArH), 8.17 (d, 1H, ArH), 8.43 (s, 1H, ArH), 8.60 (d, 1H, ArH), 8.75 (d, 1H, ArH), 10.32 (s, 1H, NH)	519	49,900
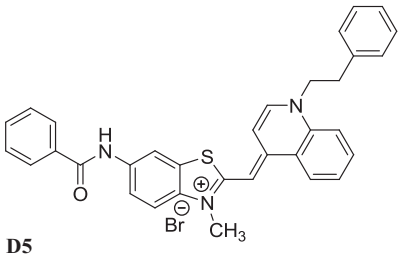 **D5**	3.20 (t, 2H, CH_2Ph), 4.03 (s, 3H, NCH_3), 4.84 (t, 2H, NCH_2), 6.91 (s, 1H, CH), 7.20–7.31 (m, 6H, ArH), 7.58 (t, 2H, ArH), 7.64 (t, 1H, ArH), 7.76 (t, 1H, ArH), 7.82 (d, 1H, ArH), 7.89 (dd, 1H, ArH), 7.99–8.02 (m, 3H, ArH), 8.22 (d, 1H, ArH), 8.32 (d, 1H, ArH), 8.59 (d, 1H, ArH), 8.79 (d, 1H, ArH), 10.60 (s, 1H, NH)	519	77,900
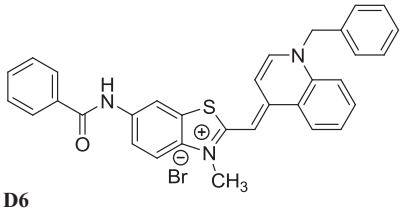 **D6**	4.12 (s, 3H, NCH_3), 5.92 (s, 2H, CH2), 7.03 (s, 1H, CH), 7.36–7.40 (q, 3H, ArH), 7.45 (t, 2H, ArH), 7.49 (d, 1H, ArH), 7.63 (t, 2H, ArH), 7.70 (t, 1H, ArH), 7.75 (t, 1H, ArH), 7.93 (t, 2H, ArH), 7.98 (dd, 1H, ArH), 8.01 (d, 1H, ArH), 8.06 (d, 2H, ArH), 8.70 (d, 1H, ArH), 8.82–8.85 (q, 2H, ArH), 10.69 (s, 1H, NH)	519	73,600

Table 1 (*Continued*)

Dye structures	^{1}H NMR, 600 MHz, DMSO-d_6 δ [ppm]	λ_{max} [nm]	ε [l mol^{-1} cm^{-1}]
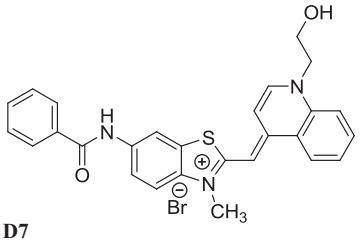 **D7**	3.84 (q, 2H, CH_2OH), 4.03 (s, 3H, NCH_3), 4.67(t, 2H, NCH_2), 5.15 (t, 1H, OH), 6.91 (s, 1H, CH), 7.37 (d, 1H, ArH), 7.57 (t, 2H, ArH), 7.64 (t, 1H, ArH), 7.75 (t, 1H, ArH), 7.80 (d, 1H, ArH), 7.89 (dd, 1H, ArH), 7.95–8.01 (m, 3H, ArH), 8.16 (d, 1H, ArH), 8.49 (d, 1H, ArH), 8.58 (s, 1H, ArH), 8.80 (d, 1H, ArH), 10.59 (s, 1H, NH)	516	61,900
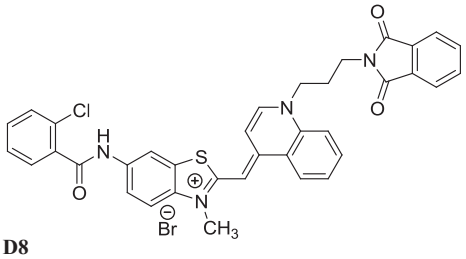 **D8**	2.16 (m, 2H, CH_2), 3.69 (t, 2H, NCH_2), 3.93 (s, 3H, NCH_3), 4.61 (t, 2H, CH_2N), 6.81 (s, 1H, CH), 7.22 (d, 1H, ArH), 7.44 (t, 1H, ArH), 7.48–7.50 (m, 1H, ArH), 7.54–7.62 (m, 2H, ArH), 7.67 (t, 1H, ArH), 7.71–7.73 (m, 1H, ArH), 7.77–7.82 (m, 5H, ArH), 7.91 (t, 1H, ArH), 8.10 (t, 1H, ArH), 8.52 (d, 1H, ArH), 8.57 (d, 1H, ArH), 8.70 (d, 1H, ArH), 10.84 (s, 1H, NH)	519	64,000
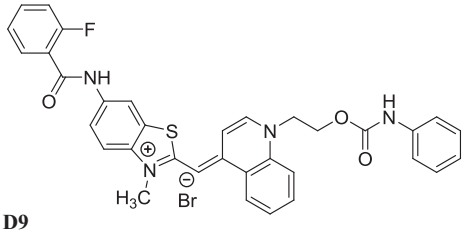 **D9**	4.04 (s, 3H, NCH_3), 4.56 (t, 2H, NCH_2), 4.91 (t, 2H, CH_2O), 6.92 (s, 1H, CH), 6.96 (t, 1H, ArH), 7.23 (t, 2H, ArH), 7.31 (d, 1H, ArH), 7.36–7.40 (m, 4H, ArH), 7.61–7.64 (q, 1H, ArH), 7.71–7.76 (m, 2H, ArH), 7.81 (t, 2H, ArH), 7.98 (t, 1H, ArH), 8.20 (d, 1H, ArH), 7.51–8.56 (m, 2H, ArH), 8.79 (d, 1H, ArH), 9.71 (s, 1H, NH), 10.79 (s, 1H, NH)	519	75,300
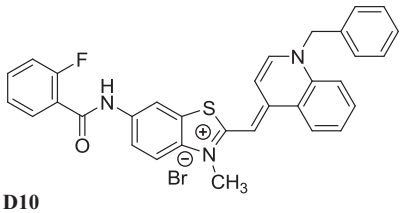 **D10**	4.06 (s, 3H, NCH_3), 5.87 (s, 2H, CH_2), 6.98 (s, 1H, CH), 7.30–7.34 (m, 2H, ArH), 7.37–7.40 (m, 4H, ArH), 7.43 (d, 1H, ArH), 7.61–7.67 (m, 1H, ArH), 7.70–7.73 (m, 2H, ArH), 7.82–7.89 (m, 3H, ArH), 7.96 (d, 1H, ArH), 8.61 (s, 1H, ArH), 8.79 (t, 2H, ArH), 10.81 (s, 1H, NH)	519	93,100
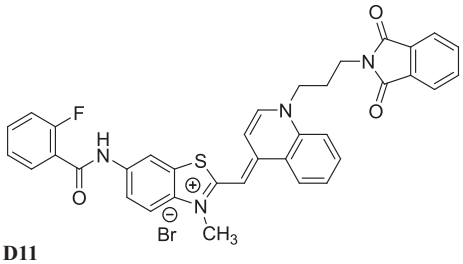 **D11**	3.76 (t, 2H, NCH_2), 4.01 (s, 3H, NCH_3), 4.66 (t, 2H, CH_2N), 6.87 (s, 1H, CH), 7.28 (d, 1H, ArH), 7.36–7.41 (m, 2H, ArH), 7.62–7.64 (m, 1H, ArH), 7.70–7.74 (m, 2H, ArH), 7.79 (s, 2H, ArH), 7.83–7.85 (m, 2H, ArH), 7.85–7.88 (m, 2H, ArH), 7.97 (t, 1H, ArH), 8.16 (d, 1H, ArH), 8.56 (s, 1H, ArH), 8.61 (d, 1H, ArH), 8.75 (d, 1H, ArH), 10.77 (s, 1H, NH)	518	68,700
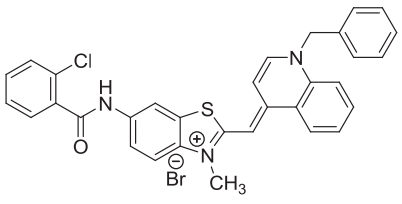 **D12**	4.06 (s, 3H, NCH_3), 5.86 (d, 2H, CH_2), 6.97 (s, 1H, CH), 7.30–7.35 (m, 3H, ArH), 7.38–7.43 (m, 3H, ArH), 7.51 (t, 1H, ArH), 7.56 (t, 1H, ArH), 7.61–7.70 (m, 3H, ArH), 7.79–7.82 (m, 1H, ArH), 7.86 (q, 2H, ArH), 7.95 (t, 1H, ArH), 8.62 (d, 1H, ArH), 8.74–8.80 (m, 2H, ArH), 10.91 (s, 1H, NH)	519	85,600

Table 1 (*Continued*)

Dye structures	^{1}H NMR, 600 MHz, DMSO-d_6 δ [ppm]	λ_{max} [nm]	ε [l mol^{-1} cm^{-1}]
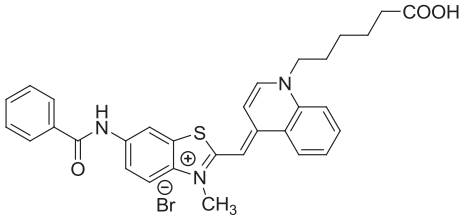 **D13**	1.36–1.41 (m, 2H, CH_2), 1.54–1.59 (m, 2H, CH_2), 1.84–1.88 (m, 2H, CH_2), 2.23 (t, 2H, CH_2), 4.03 (s, 3H, NCH_3), 4.58 (t, 2H, CH_2), 6.92 (s, 1H, CH), 7.35 (d, 1H, ArH), 7.57 (t, 2H, ArH), 7.64 (t, 1H, ArH), 7.75 (t, 1H, ArH), 7.82 (d, 1H, ArH), 7.89 (dd, 1H, ArH), 7.97–8.00 (m, 3H, ArH), 8.13 (d, 1H, ArH), 8.59–8.61 (q, 2H, ArH), 8.80(d, 1H, ArH), 10.60 (s, 1H, NH), 12.04 (brs, 1H, COOH)	517	78,900
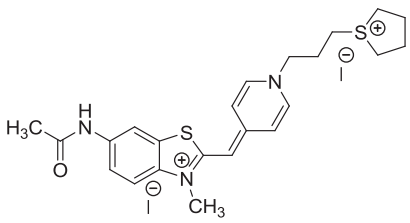 **D14**	2.17 (t, 4H, CH_2SCH_2), 2.19–2.33 (m, 4H, CH_2CH_2), 2.62 (t, 2H, S^+CH_2), 3.21–3.26 (m, 2H, CH_2), 3.43–3.53 (m, 3H, CH_3CO), 3.73 (s, 3H, NCH_3), 4.36–4.39 (q, 2H, NCH_2), 6.35 (d, 1H, CH), 7.52–7.54 (m, 2H, ArH), 7.69 (d, 1H, ArH), 7.38 (d, 1H, ArH), 7.41 (d, 1H, ArH), 8.92 (d, 1H, ArH), 9.84 (s, 1H, NH)	453	66,400
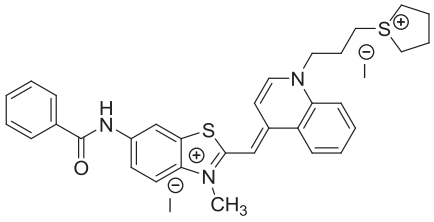 **D15**	2.10 (s, 4H, CH_2SCH_2), 2.38–2.42 (m, 4H, CH_2CH_2), 2.68 (t, 2H, S^+CH_2), 3.20–3.26 (m, 2H, CH_2), 4.36–4.39 (t, 2H, NCH_2), 6.49 (s, 1H, CH), 7.31 (d, 1H, ArH), 7.50 (t, 2H, ArH), 7.59 (t, 1H, ArH), 7.70 (t, 1H, ArH), 7.81 (d, 1H, ArH), 7.89 (dd, 1H, ArH), 7.96–8.01 (m, 3H, ArH), 8.12 (d, 1H, ArH), 8.56–8.59 (q, 2H, ArH), 8.79 (d, 1H, ArH), 9.86 (s, 1H, NH)	521	49,200
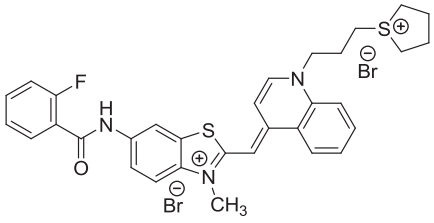 **D16**	2.08 (s, 4H, CH_2SCH_2), 2.35–2.41 (m, 4H, CH_2CH_2), 2.61 (t, 2H, S^+CH_2), 3.18–3.22 (m, 2H, CH_2), 4.31–4.36 (t, 2H, NCH_2), 6.76 (s, 1H, CH), 7.33–7.39 (m, 2H, ArH), 7.43 (d, 1H, ArH), 7.59–7.61 (m, 4H, ArH), 7.71 (t, 1H, ArH), 7.79 (d, 1H, ArH), 7.96 (d, 1H, ArH), 8.61 (s, 1H, ArH), 8.79 (t, 2H, ArH), 10.81 (s, 1H, NH)	517	58,600

Table 2
Reaction yields, melting points and elemental analysis of the examined dyes.

Dye	Molecular formulae	Mw	Yield [%]	melting point [°C]	Elemental analysis			
					N	C	S	H
					calc./found	calc./found	calc./found	calc./found
D1	$C_{34}H_{29}IN_4O_3S{\cdot}1/2CH_3OH$	716.61	53	180–183	8.00/7.82	58.29/57.82	4.58/4.47	4.17/4.36
D2	$C_{31}H_{25}BrN_4O_3S{\cdot}1/2CH_3OH$	629.54	83	184–186	9.13/8.90	60.69/60.10	5.23/5.09	4.11/4.32
D3	$C_{36}H_{29}BrN_4O_3S$	677.61	66	183–185	8.27/8.11	63.81/63.21	4.73/5.33	4.31/5.04
D4	$C_{31}H_{27}BrN_4O_3S{\cdot}CH_3OH$	647.58	75	178–180	9.10/8.65	60.49/59.35	5.21/4.95	4.42/4.83
D5	$C_{33}H_{28}BrN_3OS{\cdot}1/2CH_3OH$	610.58	41	188–190	7.07/6.88	66.66/65.90	5.39/5.25	4.75/4.95
D6	$C_{32}H_{26}BrN_3OS{\cdot}2H_2O$	580.54	96	>300	6.84/6.44	66.20/66.54	5.20/5.68	4.51/3.48
D7	$C_{27}H_{24}BrN_3O_2S$	534.47	84	275–278	7.86/7.72	60.68/60.46	6.00/6.46	4.53/5.22
D8	$C_{36}H_{28}BrClN_4O_3S$	712.05	46	175–178	7.87/7.55	60.72/60.48	4.50/4.26	3.96/4.23
D9	$C_{34}H_{28}BrFN_4O_3S{\cdot}1(1/2)H_2O$	671.58	60	180–182	8.02/7.79	58.45/58.02	4.59/5.79	4.47/5.33
D10	$C_{32}H_{25}BrFN_3OS$	598.53	43	>300	7.02/7.07	64.21/64.36	5.36/5.42	4.21/5.04
D11	$C_{36}H_{28}BrFN_4O_3S{\cdot}CH_3OH$	695.60	43	160–162	7.34/7.38	58.19/58.49	7.34/7.44	4.75/4.79
D12	$C_{32}H_{25}BrClN_3OS$	614.98	34	>300	6.83/7.26	62.50/62.30	5.21/5.62	4.10/3.08
D13	$C_{31}H_{30}BrN_3O_3S{\cdot}CH_3OH$	604.56	58	145–148	6.51/6.38	59.53/59.02	4.97/4.18	5.46/6.03
D14	$C_{23}H_{29}I_2N_3OS_2{\cdot}CH_3OH$	681.43	75	240–243	5.74/5.29	44.33/45.05	8.77/8.33	4.27/4.61
D15	$C_{32}H_{33}I_2N_3OS_2$	793.56	98	178–181	5.30/5.21	48.43/48.05	8.08/7.78	4.19/3.81
D16	$C_{32}H_{32}Br_2FN_3OS_2$	717.55	64	160–163	5.86/5.72	53.56/53.05	5.59/5.41	4.50/4.21

Table 3
Spectroscopic parameters of **D1–D16** free in TE buffer and after binding to dsDNA.

Dye	λ_{max}	λ_{max}	λ_{em}	Fluorescence intensity of free dye in TE buffer	Fluorescence intensity dye + dsDNA	Ratio
	TE buffer	TE buffer + dsDNA				
D1	507	519	547	2.98	832.51	279
D2	458	473	496	7.91	128.06	16
D3	517	530	547	8.35	446.34	53
D4	518	521	545	1.68	74.66	69
D5	509	520	546	1.31	223.52	170
D6	500	520	545	1.29	348.22	270
D7	503	516	546	2.02	695.58	344
D8	504	519	543	0.89	383.41	383
D9	508	519	544	1.12	998.80	892
D10	501	519	545	0.96	992.15	1033
D11	512	525	545	2.09	710.18	340
D12	512	519	543	0.98	817.24	834
D13	509	512	543	2.45	941.71	385
D14	451	465	496	8.79	770.15	88
D15	509	512	549	0.99	183.86	186
D16	510	516	547	0.80	349.32	437

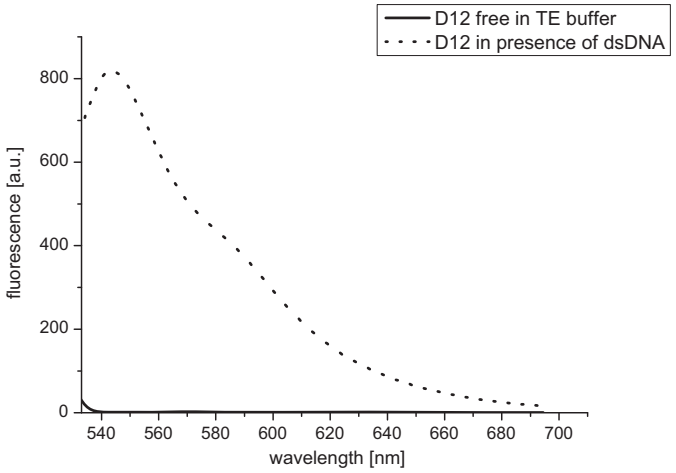

Fig. 1. Fluorescence intensity of **D12** free in TE buffer and after binding to dsDNA.

Table 4
Parameters of cyanine–DNA binding calculated using McGhee & von Hippel model.

Dye	K, $\times 10^5$, M^{-1}	n	a, $\times 10^3$, M^{-1}
D1	0.66 ± 0.15	2.49 ± 0.74	1.21 ± 0.36
D2	2.13 ± 0.63	1.49 ± 0.44	0.16 ± 0.04
D3	0.48 ± 0.14	1.95 ± 0.58	1.17 ± 0.35
D4	2.37 ± 0.71	1.81 ± 0.54	0.39 ± 0.11
D5	0.23 ± 0.07	1.05 ± 0.31	8.37 ± 2.51
D6	2.08 ± 0.62	1.51 ± 0.45	0.38 ± 0.11
D7	0.47 ± 0.14	1.05 ± 0.31	8.05 ± 2.41
D8	1.20 ± 0.36	2.49 ± 0.74	1.29 ± 0.38
D9	2.32 ± 0.69	3.24 ± 0.97	1.35 ± 0.40
D10	0.53 ± 0.15	2.99 ± 0.89	5.22 ± 1.56
D11	0.98 ± 0.29	3.00 ± 0.9	1.31 ± 0.39
D12	0.79 ± 0.23	4.79 ± 1.43	10.6 ± 3.1
D13	1.19 ± 0.35	3.19 ± 0.95	1.78 ± 0.53
D14	7.58 ± 2.27	3.13 ± 0.93	3.66 ± 1.09
D15	0.55 ± 0.16	3.19 ± 0.95	1.62 ± 0.48
D16	1.27 ± 0.38	1.57 ± 0.47	2.56 ± 0.76

the highest n and a, while **D14** has the largest K value. This finding can be explained by the fact that the association constant reflects the strength of binding, while the term "molar fluorescence" can be roughly related to the sensitivity of the dye to DNA. Specifically, the binding constant is determined by molecular interactions (e.g. hydrophobic, ionic, van der Waals, H-bonding, etc.) stabilizing complex formation. Molar fluorescence, in turn, is an inherent spectroscopic characteristic of the dye, proportional to quantum yield and determined by the ability of the fluorophore to respond to the changes in its microenvironment [19].

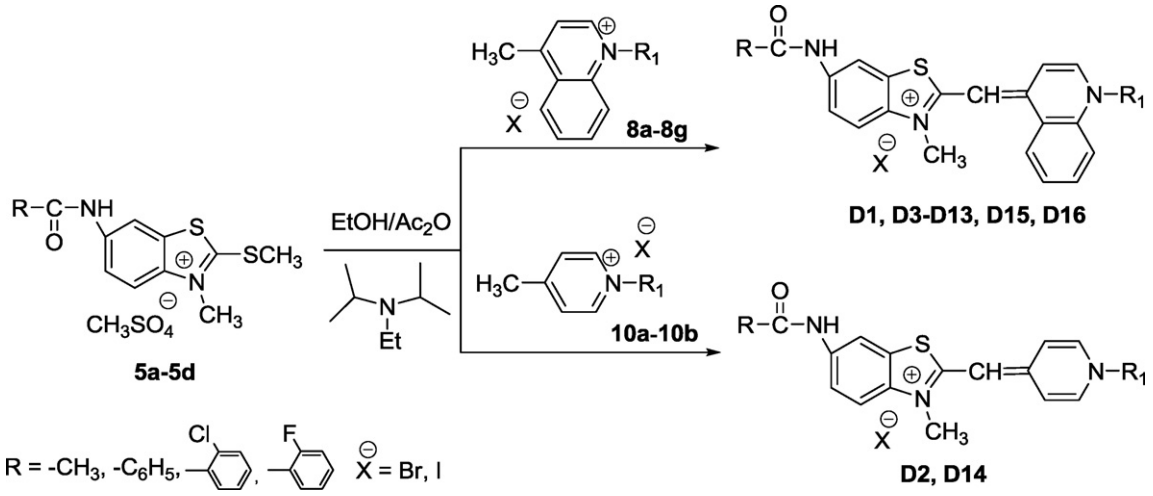

Scheme 4. Synthesis of novel monomethine cyanine dyes **D1**–**D16**.

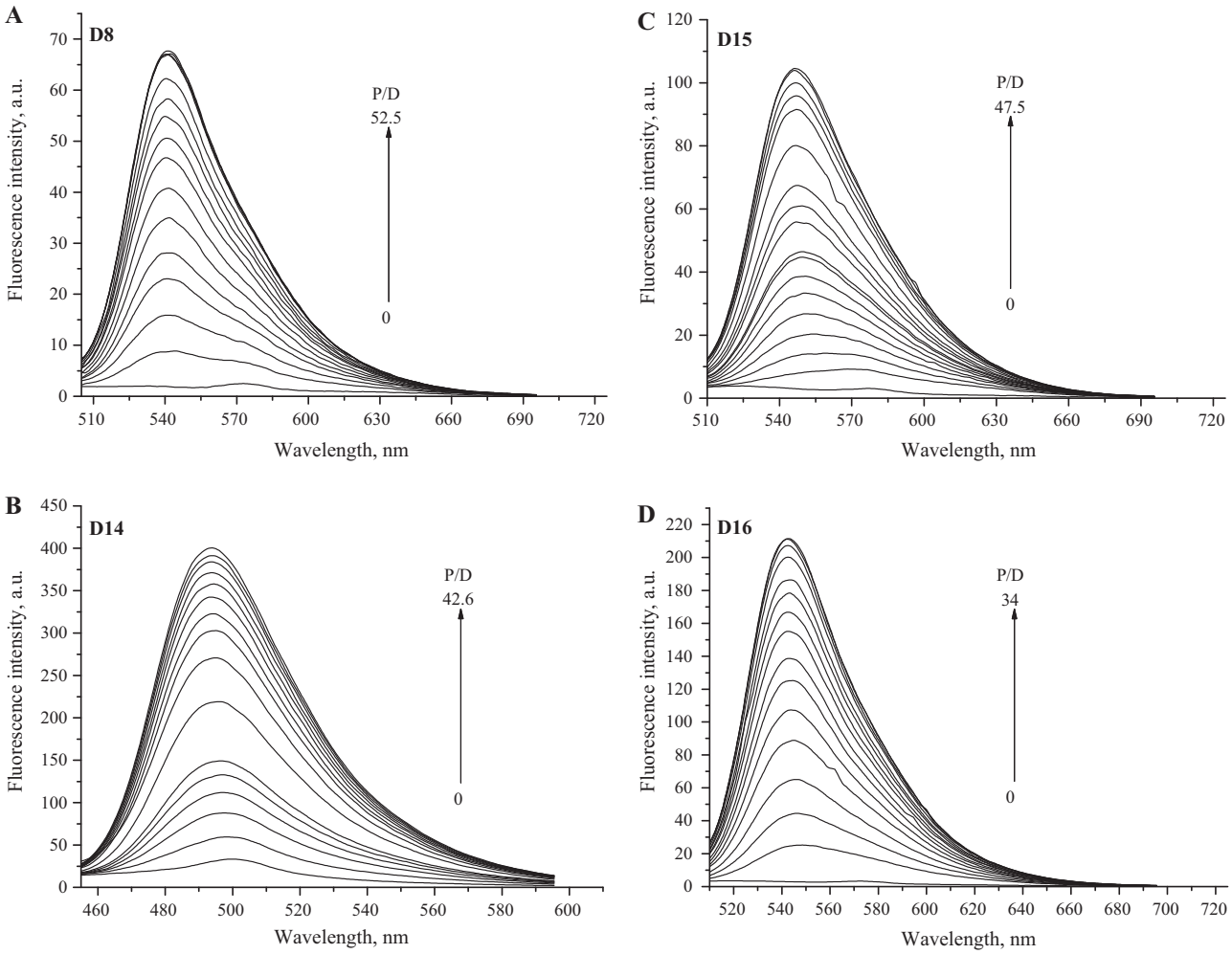

Fig. 2. Representative fluorescence spectra of cyanine dyes bound to dsDNA.

Below we analyse the molecular events that underlie complex formation between DNA and cyanines. The relative affinity of the dyes for nucleic acids is largely determined by the nature of their association. Generally, three main modes of interaction between guest molecules and DNA occur: (i) intercalation, (ii) minor groove binding, and (iii) major groove binding. While the latter mode is specific mainly for large macromolecules such as proteins, intercalation and minor groove binding represent the most common pathways of DNA complexation with small molecules. Intercalation is typical for planar aromatic cationic molecules. This type of binding results from the incorporation of a dye planar aromatic moiety between the DNA base pairs, followed by unwinding and lengthening of the DNA helix. In contrast, groove binders are crescent-shaped heteroaromatic structures possessing conformational flexibility which allows the dye molecule to adjust in the DNA groove. Compared to intercalation, groove binding distorts native DNA conformation to a lesser extent. Unfortunately, these two modes of dye–DNA interaction cannot be distinguished by fluorescence spectroscopy. A distinction can only be made if more sophisticated techniques such as ^{31}P NMR, ^{1}H NMR or circular and linear dichroism are employed [8]. However, detailed analysis of the available literature on DNA interactions with fluorophores allowed us to suggest that the preferential mode of cyanine binding to DNA in our case is intercalation. This assumption was based on the following considerations. Firstly, the geometric evidence is consistent with this statement. The diameter of dsDNA is 2 nm so the space available for intercalation is also about 2 nm. The sizes of dyes **D1**–**D16** were estimated to be 1.8–2.2 nm, which constitutes an ideal fit for the DNA geometry. Secondly, for minor groove binding to occur, the dye should possess the degree of flexibility which is more usual in polymethines [1]. Thirdly, typical binding constants for organic dye–DNA complexation via intercalation fall in the range 10^4–10^5 M^{-1}, and are usually much smaller than those observed for groove binders (10^5–10^6 M^{-1}) [8]. As shown in Table 4, association constants for dyes **D1**–**D16** vary from 2.27×10^4 to 7.58×10^5, lending additional support to the intercalative binding mode. Finally, for 11 probes the derived value of n is about 2, the magnitude obeying the "neighbour exclusion principle" of intercalation which says that the binding of one intercalating molecule between two DNA base pairs hinders access of the next binding site to another intercalator [1,8]. Exceptions are only **D9**, **D11**–**D14**. Site exclusion parameters for these dyes have values ranging from 3 to 4.8. To conclude, to determine whether it is indicative of another binding mode or a simple mathematical artefact, additional experiments are needed.

To summarize, the present work was undertaken to evaluate the potential of novel asymmetric cyanine dyes to act as non-covalent DNA labels. The dyes were found to have negligible fluorescence in the free state, but exhibited a significant emission increase upon DNA binding. The dyes **D9**, **D10**, **D12** and **D16** showed the most pronounced fluorescence enhancement. This preferential property

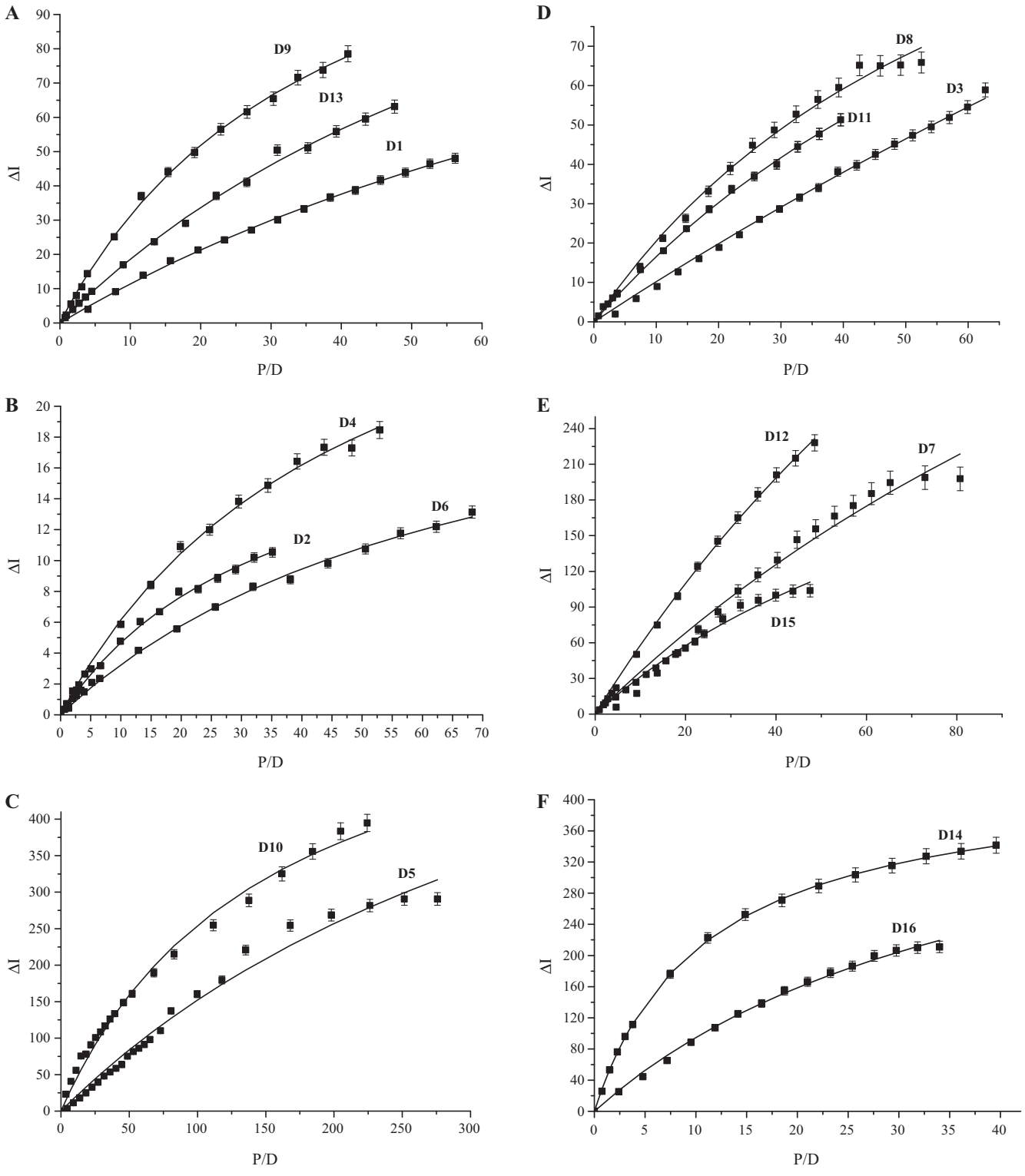

Fig. 3. Isotherms of binding of cyanine dyes **D1**–**D16** to dsDNA.

allows us to recommend these dyes as the most sensitive DNA probes.

Acknowledgements

This work was supported by the grant no. 4534 from the Science and Technology Center in Ukraine and grant no. F28.4/007 from Fundamental Research State Fund. VT gratefully acknowledges an award by Human Frontier Science Program.

References

[1] B.A. Armitage, Cyanine dye–DNA interactions: intercalation, groove binding, and aggregation, Top. Curr. Chem. 253 (2005) 55–76.

[2] D.N. Hinton, V.C. Bode, Ethidium binding affinity of circular lambda deoxyribonucleic acid determined fluorometrically, J. Biol. Chem. 250 (1975) 1061–1070.
[3] G.M. Richards, Modifications of the diphenylamine reaction giving increased sensitivity and simplicity in the estimation of DNA, Anal. Biochem. 57 (1974) 369–376.
[4] S. Nafisi, A.A. Saboury, N. Keramat, J.F. Neault, H.A. Tajmir-Riahi, Stability and structural features of DNA intercalation with ethidium bromide, acridine orange and methylene blue, J. Mol. Struct. 827 (2007) 35–43.
[5] S. Neidle, L.H. Pearl, P. Herzyk, H.M. Berman, A molecular model for proflavine-DNA intercalation, Nucleic Acids Res. 16 (1988) 8999–9016.
[6] G.A. Daxhelet, M.M. Coene, P. Hoet, C.G. Cocito, Spectrofluorometry of dyes with DNAs of different base composition and conformation, Anal. Biochem. 179 (1989) 401–403.
[7] T.G. Deligeorgiev, S. Kaloyanova, J.J. Vaquero, Intercalating cyanine dyes for nucleic acid detection, Recent Pat. Mater. Sci. 2 (2009) 1–26.
[8] H. Ihmels, D. Otto, Intercalation of organic dye molecules into double-stranded DNA – general principles and recent developments, Top. Curr. Chem. 258 (2005) 161–204.
[9] V.B. Kovalska, M.Y. Losytskyy, S.M. Yarmoluk, Luminescence spectroscopic studies of trimethinecyanines substituted in polymethine chain with nucleic acids and proteins, Spectrochim. Acta A 60 (2004) 129–136.
[10] B. Kovalska, K.D. Volkova, M.Y. Losytskyy, O.I. Tolmachev, A.O. Balanda, S.M. Yarmoluk, 6,6′-Disubstituted benzothiazole trimethine cyanines–new fluorescent dyes for DNA detection, Spectrochim. Acta A 65 (2006) 271–277.
[11] S.M. Yarmoluk, V.B. Kovalska, M.Y. Losytskyy, Symmetric cyanine dyes for detecting nucleic acids, Biotech. Histochem. 83 (2008) 131–145.
[12] J.T. Petty, J.A. Bordelon, M.E. Robertson, Thermodynamic characterization of the association of cyanine dyes with DNA, J. Phys. Chem. B 104 (2000) 7221–7227.
[13] L.G.S. Brooker, G. Keyes, W. Williams, Color and constitution. V.[1] The absorption of unsymmetrical cyanines. Resonance as a basis for a classification of dyes, J. Am. Chem. Soc. 64 (1942) 199–209.
[14] T. Deligeorgiev, S. Kaloyanova, N. Lesev, J.J. Vaquero, An easy and fast ultrasonic selective S-alkylation of hetaryl thiols at room temperature, Ultrason. Sonochem. 17 (2010) 783–788.
[15] (a) A.I. Vogel, Vogel's textbook of practical organic chemistry, in: B.S. Furniss, A.J. Hannaford, P.W.G. Smith, A.R. Tatchell, (Eds.), Longman Scientific & Technical (1989), p. 909; (b) A.I. Vogel, Vogel's textbook of practical organic chemistry, in: B.S. Furniss, A.J. Hannaford, P.W.G. Smith, A.R. Tatchell, (Eds.), Longman Scientific & Technical (1989), p. 1159.
[16] T. Deligeorgiev, N. Gadjev, A. Vasilev, K.-H. Drexhage, S.M. Yarmoluk, Synthesis of novel monomeric and homodimeric cyanine dyes with thioacetyl substituents for nucleic acid detection, Dyes Pigments 72 (2007) 28–32.
[17] N.I. Gadjev, T. Deligeorgiev, S.H. Kim, Preparation of monomethine cyanine dyes as noncovalent labels for nucleic acids, Dyes Pigments 40 (1999) 181–186.
[18] T. Deligeorgiev, I. Timtcheva, V. Maximova, N. Gadjev, K.-H. Drexhage, Fluorescence characteristics of variously charged asymmetric monomethine cyanine dyes in the presence of nucleic acids, J. Fluorescence 12 (2002) 225–229.
[19] B. Valeur, Molecular Fluorescence. Principles and Applications, Wiley-VCH, New York, 2002.